

Numerical study of shear lag of high strength steel bolted and welded angles

*Y.H. Xiong¹⁾, Angus C.C. Lam²⁾, Michael C.H. Yam³⁾, and K.F. Chung⁴⁾

^{1), 3)} *Department of Building and Real Estate,*

The Hong Kong Polytechnic University, Hong Kong, China

²⁾ *Department of Civil and Environmental Engineering, University of Macau, China*

⁴⁾ *Department of Civil and Environmental Engineering,
The Hong Kong Polytechnic University, Hong Kong, China*

¹⁾ 13902414r@connect.polyu.hk

ABSTRACT

This paper presents a numerical study of the shear lag effects on high strength steel (HSS) bolted and welded single angles by the finite element method. The finite element models used in the study were calibrated by the test results of normal strength steel angles subjected to tension. In total, fourteen HSS angles were simulated and typical HSS material properties used in the analysis were obtained from the literature. The parameters examined in the study included the connection length and the connection eccentricity. It is observed that the tensile capacity and final elongation of the HSS angles are considerably lower than those of the corresponding normal steel angles. The widely used $1 - \bar{x}/L$ rule in general overestimated the capacities of the HSS bolted single angles but provided conservative estimates of the capacities of the welded ones examined in this study.

1. INTRODUCTION

In the past few years, high strength steels (HSS) have gained increasing attention in civil engineering industry due to its cost-effective characteristic. Compared to mild steels, HSS leads to smaller size structural components, thereby reducing the cost of fabrication, transportation and erection. In addition, HSS structures are more environmentally sustainable due to less consumption of steel (Hajjar et al. 1997). Furthermore, with the improvement of TMCP (Thermo-Mechanical Control Process) technology, which allows the production of high strength steels with high toughness, weldability, cold formability and corrosion resistance (Raoul 2005), the potential use of HSS in common civil engineering constructions in the future is promising. Although HSS has already been applied in structures such as bridges, stadiums and transmission towers since 1960s (Shi et al. 2012), there are a number of problems need to be investigated. One important issue is the influence of lower ductility of HSS material. It is well known that HSS has much lower ductility than normal structural steels. For instance, the strain

¹⁾ Graduate Student

²⁾ Assistant Professor

³⁾ Associate Professor

⁴⁾ Professor

at the tensile strength (ϵ_u) of typical S690 and S275 steel is about 7% and 20%, respectively. This difference of ductility will undoubtedly result in different structural behaviours of tension members.

In this paper, the shear lag effect of HSS bolted and welded single angles are studied. The shear lag effect is the influence of the fact that angles are often connected by only one leg, hence, the unconnected leg's deformation lags behind the connected leg and thereby the stresses correspondingly decrease from the connected heel to the extreme outstanding toe. This non-uniform stress distribution will undoubtedly reduce the tensile capacity of the angles. Shear lag effect is commonly considered by many specifications such as the AISC-LRFD, CSA/CAN-S16-01 and EN-1993-1-8:2005 using a reduction factor. However, all the equations adopted are based on behaviours of test specimens made of normal structural steels. In fact, the shear lag effect is expected to be more significant when HSS is used instead of normal structural steels because when the ductility of the material is lower, premature fracture of the connected leg may occur and hence the effectiveness of the unconnected leg is reduced which leads to a reduction in tensile capacity. Therefore, the applicability of the current shear lag design equations to HSS tension members should be examined.

Many researchers have investigated the shear lag effect of bolted or welded angles. The mostly widely used equation was proposed by Munse and Chesson (1963) and was adopted in AISC-LRFD and CSA/CAN-S16-01:

$$U = 1 - \bar{x}/L(1)$$

Where U = shear lag factor, \bar{x} = connection eccentricity and L =length of connection.

This equation was developed based on about 1000 riveted and bolted connection specimens (Munse and Chesson, 1963). Although the equation was mainly derived from bolted connection tests, this equation is also treated as applicable to welded connections. Other relevant researches include (Nelson 1953, Kulak and Wu 1993, Orbison and Barth 2002) for bolted connections and (Davis and Boomsliker 1934, Gibson and Wake 1942, Regan and Salter 1984, Easterling and Gonzalez 1993, Zhu et al. 2009, Fang et al. 2013) for welded connections. However, almost all of these investigations focused on the normal steels. Fang et al. (2013) made an attempt to study the shear lag effect of HSS angles. Two out of twelve welded single angles were made of steels with yield strength of 484 MPa and ultimate strength of 693 MPa. The test efficiency (defined as the ratio of ultimate capacity to the calculated tensile capacity of the gross section) of specimens fabricated using HSS was much lower than that of specimens fabricated using mild steels. Moreover, the predicted values by various specifications were found unconservative. Therefore, more experimental and numerical research works are required for a better understanding of the shear lag of HSS angles. The main objective of this research is to establish a numerical model to investigate the behaviours of HSS bolted and welded single angles. The emphasis is to compare the structural behaviour of HSS and normal structural steel angles subject to tension. In addition, the influence of connection length and connection eccentricity is considered. Finally, the widely used design equation $U = 1 - \bar{x}/L$ is further examined.

2. NUMERICAL ANALYSIS

The commercial finite element program ABAQUS version 6.12 is used for the numerical analysis of the HSS angle tension members. Both the material and geometry nonlinear effects are taken into account. The experimental data from Zhu et al. (2009) and Kulak et al. (1997) were used for the validation of the models of welded and bolted angle tension members, respectively.

2.1 Finite element model

The typical finite element models (FEM) of bolted and welded angle members are shown in Figure 1 and Figure 2, respectively. Only half of each specimen is modelled due to symmetry. At the mid-length of each specimen, the x-direction translational degree of freedom (DOF) and the rotational DOF about the y, z axes are constrained. The leading edge of the gusset plate is constrained in all directions except the longitudinal direction. At the leading edge, a longitudinal uniform displacement is applied as the axial load. The angle, gusset plate, bolts and welds are all modelled as 3D deformable solid parts and meshed by 3-D, 8-node linear brick, reduced integration, hourglass control elements (C3D8R). The interaction between all surface-to-surface pairs is assigned as a general contact with “hard” contact in normal behaviour and the penalty friction formulation in tangential behaviour. The friction coefficient is taken as 0.25 which is the measured average nominal coefficient of various steels (Vasarhelyi et al. 1967). To model the real bolt-hole bearing condition, a 2mm clearance between the bolt shank and the bolt hole is included in the model. Preloads are applied on each bolt by the command “bolt force”. The quantity of preload is taken as 70% of the bolts’ tensile strength. As for the welded connection, the “tie” constraints are prescribed among all the parts.

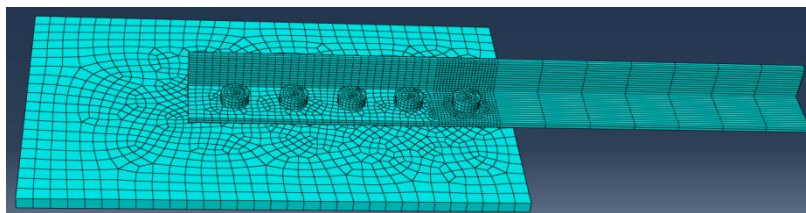


Figure 1 Typical FEM of bolted angle members

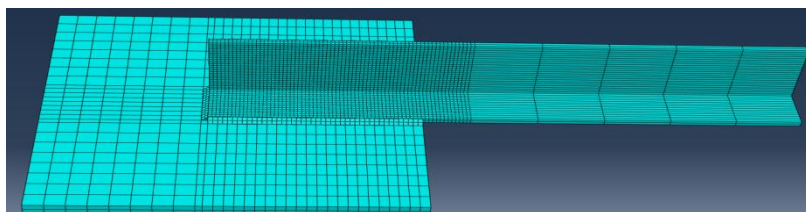


Figure 2 Typical FEM of welded angle members

2.2 Material property

An isotropic-hardening elastic-plastic material model with von Mises yield criterion is used. The stress-strain relationship is modelled by a multi-linear stress-strain curve and the true stress and true strain are input to the models. Young's modulus is taken as 210,000 MPa and the Poisson's ratio is 0.3. In order to model the fracture behaviour of the steel material, the command "damage initial" and "damage evolution" is employed. The damage occurs when the maximum tensile stress of material is reached. Then the stress will decrease according with the material property from ultimate stress to zero. And the element will be removed when the stress becomes zero.

2.3 Model validation

The test data of specimen S5 and S9 from Kulak et al. (1997) and specimen A1-200US and A1-200UL from Zhu et al. (2009) were used to validate the finite element models of the bolted and welded connections, respectively. The details of the specimens for validation are shown in Table 1. The comparison of the numerical and the experimental results are shown in Table 2 and the load-elongation curves are shown in Figure 3.

As shown in Figure 3, the load-elongation curves of the finite element analysis (FEA) results are in good agreement with those from the tests. The ratio of the FEM results to the experimental results ranges from 0.96 to 0.99 with an average ratio of 0.97 and a coefficient of variation of 0.013. The validated FE models were subsequently used to analyse the shear lag of HSS angles.

Table 1 Details of specimens for validation

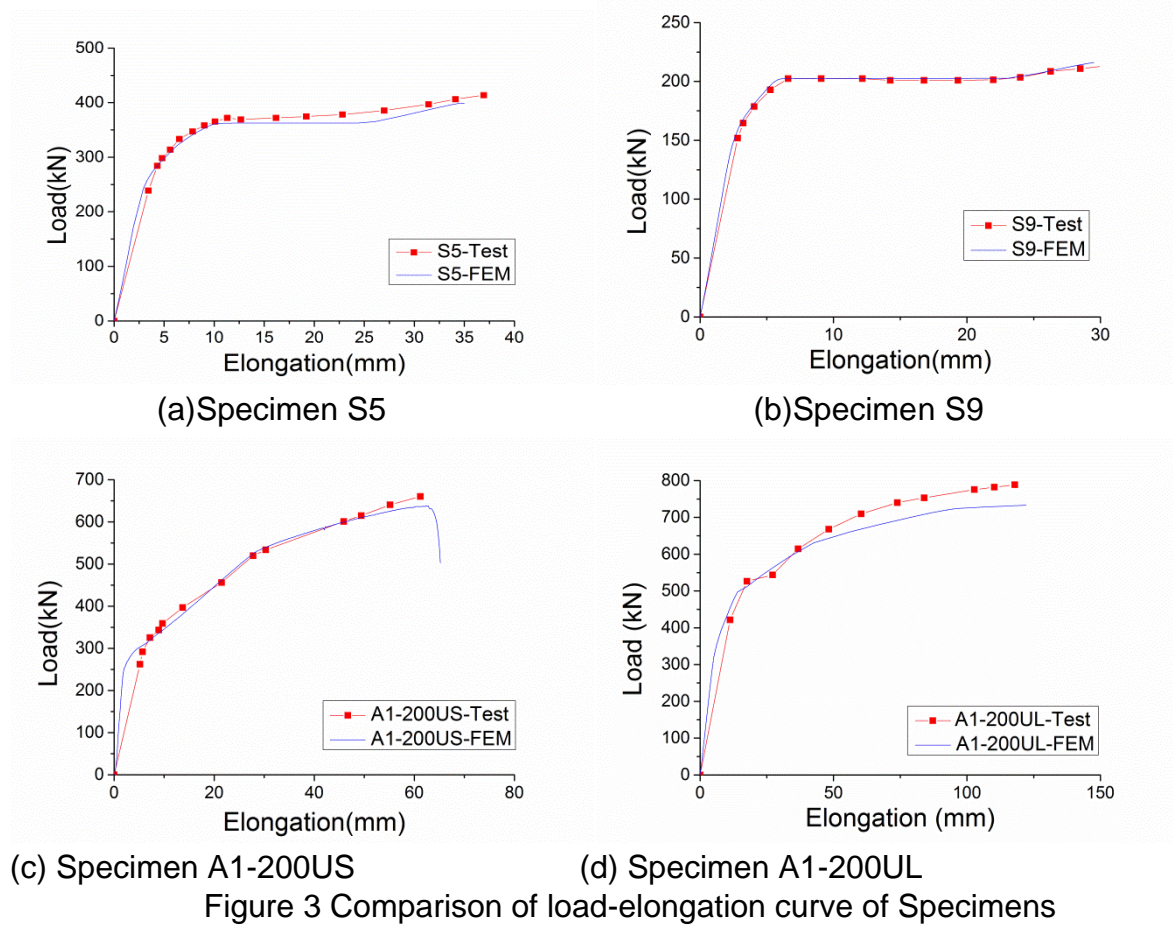
Specimen	Angle size (mm)	Connected leg (mm)	Number of bolts	Bolt spacing (mm)	Weld length (mm)
S5	102×76×6.4	102	6	76	—
S9	76×51×4.8	76	6	76	—
A1-200US	125×75×10	75	—	—	200
A1-200UL	125×75×10	125	—	—	200

Table 2 Comparison of experimental and FEA results

Specimen	Experiment ¹ (kN)	FEA (kN)	FEA/Experiment
S5	217.5	216.2	0.99
S9	413.6	399.2	0.97
A1-200US	665.0	638.0	0.96
A1-200UL	760.0	733.0	0.96

Notes:

1. The experimental ultimate load is the static ultimate load.



2.4 Parametric study

A total of 9 bolted and 9 welded single angle tension members were simulated. For each connection type, seven members were modelled with S690 steel and the remaining two members were modelled using S275 steel. Table 3 and Table 4 summarize the engineering material property and true stress-strain data, respectively. The details of the bolted and welded members are illustrated in Table 5 and Table 6, respectively. All the section sizes used for the members were selected from the Guide to BS: 5950-1:2000. The parameters considered in the study are steel grade, connection eccentricity (by varying section size and connected leg) and connection length (by varying spacing between bolts or longitudinal weld length).

Table 3 Engineering material property

Steel grade	Elastic modulus (MPa)	Yield stress (MPa)	Ultimate stress (MPa)	Strain at ultimate stress (%)
S690	210400	781	822	5.0
S275	203806	268	418	25.0

Table 4 True stress-strain data used in the model

Steel S690 ¹		Steel S275 ²	
σ_{true} (MPa)	ϵ_{true}^p	σ_{true} (MPa)	ϵ_{true}^p
781	0.0000	264	0.0000
821	0.02567	265	0.0027
860	0.04593	268	0.0086
		283	0.0135
		348	0.0376
		419	0.0930
		445	0.1375
		476	0.1798
		480	0.2205

Note:

1. The data of S690 steel is from authors' information.
2. The data of S275 steel is from Zhu et al. (2009).

3. RESULTS AND DISCUSSION

3.1 General

The failure mode of bolted and welded angle members as illustrated in Figure 4 is section fracture near the connection as expected. For the members with the bolted connections, angle-fracture occurs in the vicinity of the inner first bolt hole due to stress concentration and then propagates across the width of the connected leg. For the welded connections, angle-fracture occurs near the toe of the connected leg and propagates to the heel at the critical section. The efficiencies (the ratio of FE tensile capacity to the calculated tensile capacity) of all the specimens are summarized in Table 5 and Table 6.

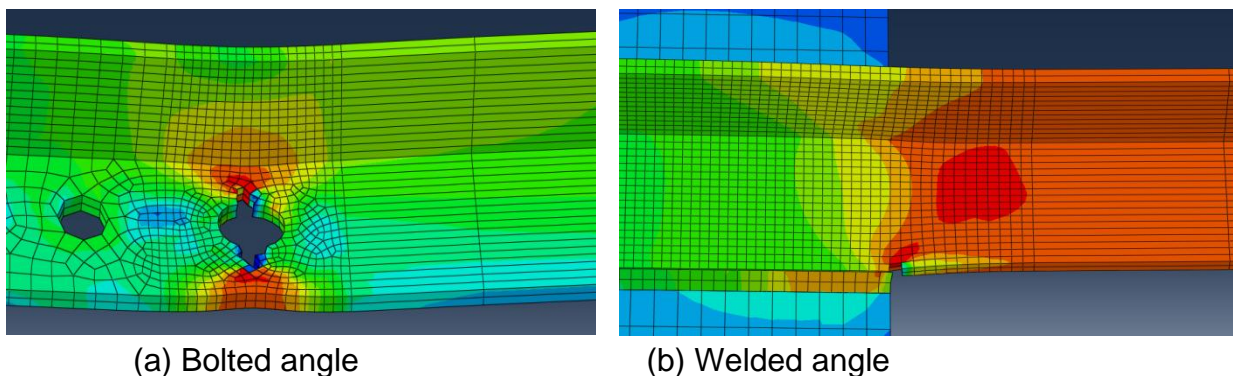


Figure 4 Typical fracture modes of bolted and welded angles

Table 5 Specimen details and FEA results of bolted specimens

Specimen	Angle size (mm)	Steel grade	Angle length (mm)	Connected leg length (mm)	No. of bolts	Bolt spacing (mm)	$F_u A_n$ (kN)	P_{FEM} (kN)	$\frac{P_{FEM}}{F_u A_n}$ (%)	$\frac{P_{rule}^1}{F_u A_n}$ (%)	$\frac{P_{FEM}}{P_{rule}}$ (%)
A1-60L	80*60*8	S690	1520	80	5	60	709	543	76.6	93.8	81.7
A1-75L	80*60*8	S690	1640	80	5	75	709	562	79.2	95.0	83.4
A1-90L	80*60*8	S690	1760	80	5	90	709	585	82.5	95.8	86.2
A1-75S	80*60*8	S690	1640	60	5	75	709	468	66.0	91.7	72.0
A2-60S	100*65*8	S690	1520	65	5	60	874	500	57.2	86.3	66.3
A2-75S	100*65*8	S690	1640	65	5	75	874	512	58.6	89.0	65.8
A2-90S	100*65*8	S690	1760	65	5	90	874	526	60.2	90.8	66.3
B1-75L	80*60*8	S275	1640	80	5	75	361	311	86.3	95.0	91.0
B2-75S	100*65*8	S275	1640	65	5	75	445	321	72.1	91.7	78.6

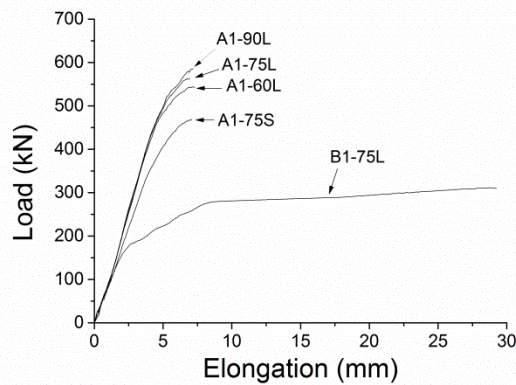
Table 6 Specimen details and numerical results of welded specimens

designatio n	Angle size (mm)	Steel grade	Angle length (mm)	Connected leg length (mm)	Connection Length (mm)	$F_u A_g$ (kN)	P_{FEM} (kN)	$\frac{P_{FEM}}{F_u A_g}$ (%)	$\frac{P_{rule}}{F_u A_g}$ (%)	$\frac{P_{FEM}}{P_{rule}}$ (%)
C1-220L	80*60*8	S690	1240	80	220	867	842	97.1	93.2	104.2
C1-300L	80*60*8	S690	1400	80	300	867	845	97.5	95.0	102.6
C1-380L	80*60*8	S690	1560	80	380	867	847	97.7	96.1	101.7
C1-300S	80*60*8	S690	1400	60	300	867	792	91.3	91.7	99.6
C2-220S	100*65*8	S690	1240	65	220	1031	822	79.7	85.0	93.8
C2-300S	100*65*8	S690	1400	65	300	1031	869	84.2	89.0	94.6
C2-380S	100*65*8	S690	1560	65	380	1031	906	87.9	91.3	96.3
D1-300L	80*60*8	S275	1400	80	300	441	417	94.5	95.0	99.5
D2-300S	80*60*8	S275	1400	65	300	525	486	92.6	89.0	104.0

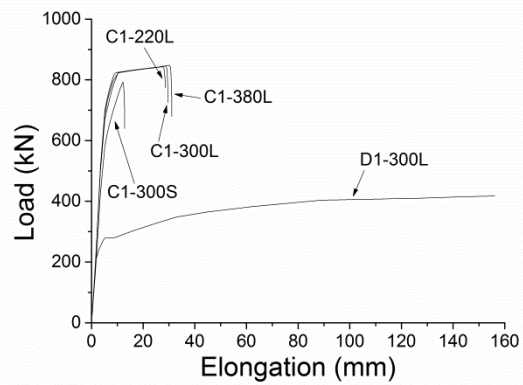
Note: 1. P_{rule} indicates the predicted capacity by the $1 - \bar{x}/L$ rule.

3.2 Load-elongation response

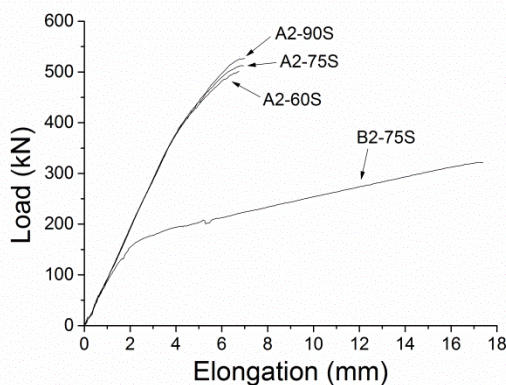
As the applied load increases, the angle starts to bend due to the out-of-plane eccentricity. The axis of loading gradually approaches the centroid axis of the angle, leading to an eventual alignment of the two loading axes. The load-elongation curves of all the members are shown in Figure 5. It is observed that the elongations of the normal steel angle members are substantially higher than those of the HSS angle members due to the lower ductility of HSS material. In the elastic range, the initial stiffness of HSS angles and normal steel angles are almost the same. For the normal steel angles, inelastic behaviour occurs early when the elongation only reaches about 5% of the final elongation. By contrast, for the HSS angles, the point where inelastic behaviour occurs is 30%~60% of the final elongation.



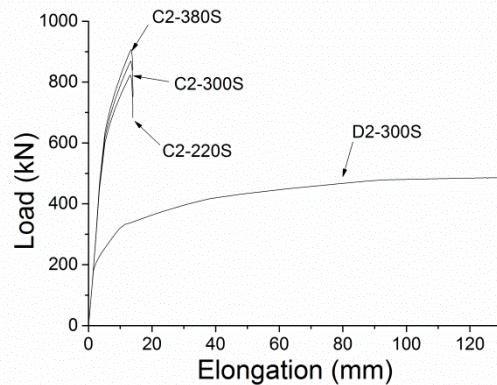
(a) Specimen A1, B1



(b) Specimen C1, D1



(c) Specimen A2, B2



(d) Specimen C2, D2

Figure 5 Load-elongation curves

3.3 Effect of steel grade

In terms of the bolted angle members, the effect of steel grade on shear lag can be seen by comparing the two groups: A1-75L and B1-75L for the long leg connection and A2-75S and B2-75S for the short leg connection. The difference between the efficiency

of angle A1-75L and angle B1-75L is 7.1% and the efficiency of angle A2-75S is 13.5% lower than that of angle B2-75S. It can be seen that the steel grade strongly influences the shear lag effects of bolted angle members. The efficiency of the angle members decreases with decreasing material ductility. In particular, the efficiency of the angles connected by short leg is reduced more significantly with decreasing material ductility. As for the welded connections, when the angles are connected by the long leg, there is nearly no difference in efficiency between the HSS and normal steel angle members (97.5% for C1-300L and 94.5% for D1-300L). However, when the short leg of the welded angle member is connected to the gusset plate, the influence of ductility becomes more significant as illustrated by the efficiencies of 84.2% and 92.6% for angles C2-300S and D2-300S, respectively.

3.4 Effect of connection length and connection eccentricity

For bolted angle members, it is observed that the variation in bolt spacing does not have a significant influence on the shear lag effect regardless of whether long leg or short leg is connected. The efficiency of angles connected by long leg is 76.6%, 79.2% and 82.5% for angles A1-60L, A1-75L and A1-90L, respectively. And the efficiency of angles connected by short leg is 57.2%, 58.6% and 60.2% for angles A2-60S, A2-75S and A2-90S, respectively. As for the welded angle members, the shear lag effect of angles connected by short leg is affected more significantly than that of angles connected by long leg. For each 80mm increment of weld length, the average increase of efficiency is 4.1% for angles connected by short leg but only 0.3% for angles connected by long leg. In terms of connection eccentricity, the capacity efficiency and elongation will largely decrease with increasing connection eccentricity. For the bolted connections, the efficiency of angle members are 79.2%, 66.0% and 58.6% for angles A1-75L, A1-75S and A2-75S, respectively. For the welded connections, the efficiency of angles members are 97.5%, 91.3% and 84.2% for angles C1-75L, C1-75S and C2-75S, respectively.

3.5 Evaluation of $1 - \bar{x}/L$ rule

Comparing the FEA results with the predicted results by the $1 - \bar{x}/L$ rule, it is observed that the efficiencies of all the HSS bolted angle members are generally over-estimated by the equation. The average ratio of the FEA results to the predicted results is 83.8% and 67.6% for the long leg connected angles and short leg connected angles, respectively. As stated before, the $1 - \bar{x}/L$ rule is based on the test results of tension members made of normal steels which have relatively larger material ductility (above 20%). However, for the welded angle members, the predicted results are conservative for the long leg connected angles while only slightly unconservative for short leg connected angles with the average ratio of the FEA results to the predicted results of 96.1%.

4. SUMMARY AND CONCLUSION

A numerical study using the finite element method is employed to investigate the shear lag effect of bolted and welded single angles with high strength steel. The finite

element models are validated by the test data from other research studies. In total, nine bolted and nine welded angle members are simulated. The findings of this study are presented as follows:

1. The steel grade will largely affect the shear lag effect of bolted and welded single angles subject to tension. The elongation and section efficiency of the normal steel angles are considerably larger than those of HSS angles. The connection length does not have significant effects on the efficiency of the bolted and welded angles with long leg connection. However, the efficiency of the welded angles with short leg connection is affected by the connection length. In addition, the connection eccentricity has a great influence on the efficiency of both bolted and welded angles.
2. The $1 - \bar{x}/L$ rule provides a conservative estimate of the tension capacities of the HSS welded angles examined in this study. However, the efficiencies of HSS bolted angles are overestimated by the rule.

References

- Davis, R. P., & Boomsitter, G. P. (1934). Tensile tests of welded and riveted structural members. *Journal of the American Welding Society*, 13(4), 21-27.
- Easterling, W. S., & Gonzales, L. (1993). Shear lag effects in steel tension members. *Engineering Journal*, 3, 77-89.
- Fang, C., Lam, A. C., & Yam, M. C. H. (2013). Influence of shear lag on ultimate tensile capacity of angles and tees. *Journal of constructional steel research*, 84, 49-61.
- Gibson, G. T., & Wake, B. T. (1942). An investigation of welded connections for angle tension members. *The Welding Journal*, 44.
- Hajjar, J. F., Earls, C. J., & Gross, J. L. (1997). *Required properties of high-performance steels*. National Institute of Standards and Technology, Building and Fire Research Laboratory.
- Kulak, G. L., & Wu, E. Y. (1997). Shear lag in bolted angle tension members. *Journal of Structural Engineering*, 123(9), 1144-1152.
- Munse, W. H., & Chesson Jr, E. (1963). Riveted and bolted joints: net section design. *Journal of the Structural Division*, 89, 107-126.
- Nelson, H. M. (1953). Angles in tension. *British Constructional Steelwork Assoc. on Publication No 7, United Kingdom*, 8-18.
- Orbison, J. G., Barth, K. E., & Bartels, P. A. (2002). Net section rupture in tension members with connection eccentricity. *Journal of structural Engineering*, 128(8), 976-985.
- Regan, P. E., & Salter, P. R. (1984). Tests on welded-angle tension members. *Structural Engineer*, 62, 25-30.
- Raoul, J. (2005). *Use and application of high-performance steels for steel structures* (Vol. 8). H. P. Günther (Ed.). IABSE.
- Shi, G., Ban, H. Y., Shi, Y. J., & Wang, Y. Q. (2012). Engineering application and recent research progress on high strength steel structures. *Industrial Construction*, 42(1), 1-7.
- Vasarhelyi, D. D., & Chiang, K. C. (1967). Coefficient of friction in joints of various steels. *Journal of the Structural Division*.

Zhu, H., Yam, M. C. H., Lam, A. C. C., & Lu, V. P. (2009). The shear lag effects on welded steel single angle tension members. *Journal of Constructional Steel Research*, 65(5), 1171-1186.